Stochastic Channel Access in Underwater Networks With Statistical Interference Modeling

Zhangyu Guan, *Member, IEEE*, Hovannes Kulhandjian, *Senior Member, IEEE*, and Tommaso Melodia, *Fellow, IEEE*

Abstract—Designing efficient medium access control protocols for underwater acoustic sensor networks (UW-ASNs) is a major challenge because of the spatial and temporal interference uncertainty caused by asynchronous transmissions and by the low propagation speed of sound. To address these challenges, in this article we propose a new approach for distributed underwater medium access based on lightweight and asynchronous distributed algorithms that optimize the access probability profile over a series of time slots based on a new statistical physical interference model. The latter is based on measuring the level of interference at multiple instants of time in each time slot in order to capture the effects of temporal uncertainty and of unaligned interference. At each measurement instant, the statistical properties of time-varying interference are represented by a Gamma probability distribution. The model is validated through extensive channel measurement experiments conducted with an underwater acoustic testbed in Lake LaSalle. Based on this model, we formulate the problem of queue-aware stochastic channel access. The objective is to maximize the sum throughput of a set of concurrent and mutually interfering source-destination pairs by letting the transmitters adjust their own transmission probability profiles, without collaborating with each other, over a series of time slots *based on a statistical characterization of interference* obtained through past observations. We propose an iterative distributed solution algorithm for this problem based on a best-response strategy. At each iteration, each node individually solves a non-convex optimization problem of logarithmic complexity. The performance of the proposed distributed algorithm is evaluated by comparing it with two alternative distributed schemes and with the global optimum obtained through a newly-developed centralized globally optimal solution algorithm. Results indicate that by jointly taking the queueing and multi-slot optimization into consideration considerable improvement in terms of sum-throughput can be achieved by the proposed distributed algorithm.

Index Terms—Stochastic channel access, underwater acoustic networks, statistical interference model

1 Introduction

One of the major challenges in Underwater Acoustic Sensor Networks (UW-ASNs) [2] is to design an efficient medium access control (MAC) protocol, mainly because of the large propagation delay caused by the low propagation speed of sound in aqueous media [3]. In addition to the *temporal uncertainty* of interference caused by the asynchronous transmissions of different nodes and the time-varying wireless channels, in UW-ASNs the large (and distance-dependent) propagation delay of acoustic signals generates *spatial uncertainty*, i.e., it is hard to predict the current value of interference because acoustic signals simultaneously transmitted by different nodes located at different distances from an intended receiver do not necessarily reach the receiver at the same time [4]. As a result, in the presence of both *temporal* and *spatial uncertainty*, MAC protocols originally designed for radio-frequency (RF) in-air wireless communications cannot be efficiently applied to underwater environments directly. For example, it was shown that the benefits of synchronization of slotted ALOHA are completely lost in UW-ASNs because of the distance-dependent delay [5]. Moreover, the large propagation delay makes it challenging for transmitters to adapt to the time-varying underwater channels; since it is hard to acquire instantaneous channel state information (CSI), which is usually obtained through feedback from the receiver [6]. For the same reason, traditional carrier sensing also requires very long listen time in underwater acoustic environments, and this may significantly reduce the channel utilization [7]. Therefore, the large propagation delay imposes major challenges on underwater communications at both the transmitter and receiver sides.

Significant recent efforts have attempted to address these challenges [5], [8], [9], [10], [11], [12], [13], [14]. For example, Syed *et al.* showed in [5] that, for slotted ALOHA underwater networks, the packet collision probability can be reduced by adding a guard band to each time slot, hence limiting the negative effect of the spatial interference uncertainty.[1] In [8], Peleato and Stojanovic proposed a distance-aware collision avoidance protocol (DACAP), which uses different handshake lengths for different receivers with a potential to

- *Z. Guan is with the Department of Electrical Engineering, The State University of New York at Buffalo, Buffalo, NY 14260 USA. E-mail: guan@buffalo.edu.*
- *H. Kulhandjian is with the Department of Electrical and Computer Engineering, California State University, Fresno, Fresno, CA 93740 USA. E-mail: hkulhandjian@csufresno.edu.*
- *T. Melodia is with the Institute for the Wireless Internet of Things, Department of Electrical and Computer Engineering, Northeastern University, Boston, MA 02115 USA. E-mail: melodia@ece.neu.edu.*

Manuscript received 15 Aug. 2019; revised 15 Apr. 2020; accepted 1 May 2020. Date of publication 7 May 2020; date of current version 31 Aug. 2021.
(Corresponding author: Zhangyu Guan.)
Digital Object Identifier no. 10.1109/TMC.2020.2993026

1. A user transmitting in a given time slot might interfere with others in two consecutive time slots.

minimize the average handshake duration and hence can improve the throughput. In [9], Guo *et al.* further improved the handshaking efficiency by using an adaptive propagation-delay-tolerant collision-avoidance protocol (APCAP), which allows a node to utilize its idle time while waiting for messages to propagate. In these protocols, nodes are either required to cooperatively collect the network topology information, or to exchange handshaking signals. This may cause under-utilization of transmission time due to the inserted time guard or low-speed sound propagation in the signaling exchanges. Moreover, in heterogeneous environments, where multiple UW-ASNs coexist sharing the same spectrum, e.g., the emerging cognitive UW-ASN [15], the envisioned underwater Internet [16], and UW-ASN with jammers [17], [18], it is not that easy to implement network-wide cooperation or global synchronization for slotted channel sensing [14], especially, if the coexisting UW-ASNs are deployed and operated separately for different purposes. It is still not clear, to the best of our knowledge, how to design light-weight MAC protocols that require low signaling exchanges among competing transmissions, while considering both temporal and spatial uncertainty of interference in the underwater environments.

This paper takes a significant step in this direction by proposing a light-weight MAC that requires no signaling exchange among concurrent communication sessions, and achieves interference avoidance based on only limited local information. To be specific, we study an optimized distributed access scheme based on explicit stochastic modeling of the temporal and spatial uncertainty of interference. The main contributions of the paper are as follows.

- *Statistical Interference Modeling*. With spatial uncertainty caused by the low-speed of sound in underwater, interference observed at an intended receiver at a specific time slot may be caused by interfering transmissions originated in past time slots. This motivates us to develop a medium access scheme in which each transmitter dynamically optimizes a transmission probability profile *based on a statistical characterization of interference* obtained through its past observations, and then based on the obtained profile it decides whether to transmit or to enqueue its packets over a series of time slots. Moreover, the originated interfering signals might reach the receiver at different instants during a specific time slot. Therefore, it is insufficient to characterize interference using a single interference level for the whole time slot.

  To address these challenges, we propose an L-measurement method, which measures interference at multiple time points for each receiver in each time slot. At each measurement point, the effects of temporal uncertainty of interference, i.e., the asynchronous transmission times of different nodes or the time-varying channels, on the interference level at each measurement point are modeled using Gamma distribution functions.
- *Light-weight Channel Access*. Based on this *statistical characterization of interference*, each node is able to adapt its transmission strategy proactively to the time-varying interference to minimize the resulting packet loss rate. It is desirable for a node to transmit with high probability only in time slots when the corresponding interference levels are expected to be low, and transmit with lower probability in time slots with high interference. On the other hand, to reduce the probability that a packet needs to wait for a long time in the queue and thus becomes useless when received at the destination, a node should transmit with high probability in all time slots. By regulating the transmission probability, each transmitter should find the optimal operating point along the tradeoff between transmission and queueing to minimize its packet loss rate (and therefore to maximize the expected throughput). The channel access scheme is light weight because it requires *zero* signaling exchanges among different communication pairs.
- *Channel Access Optimization*. In the proposed light-weight MAC framework, we present a mathematical formulation of the problem of dynamic transmission strategy optimization and propose an iterative distributed solution algorithm based on a best-response strategy. At each iteration, each node individually solves a nonconvex optimization problem, in which the objective function can be transformed into a quasi-convex function so that the global optimum can be efficiently computed and solved in logarithmic time with respect to the number of jointly considered time slots. Then, the performance of the proposed distributed algorithm is evaluated by comparing it with the global optimum scheme obtained by a newly-developed centralized solution algorithm. We also validate the proposed interference model using actual underwater experiments in a lake and show that the model can capture the statistical characteristics of underwater interference well.

The core novelty of the paper lies in the formulation and analysis of a distributed MAC scheme that jointly considers the temporal and spatial uncertainty of interference in UW-ASNs. Specifically, (i) we propose the first interference model that captures the low-speed of sound propagation and time-variability of wireless underwater channels; (ii) we propose and study a framework to optimize the transmission strategy of each node based on the statistical characterization of interference while jointly considering the queueing behavior. It is worth pointing out that, since the proposed distributed MAC protocol handles the low-speed of sound in the time domain directly, its performance can further be enhanced by integrating it with MAC protocols designed based on code-division multiple access (CDMA) [19], [20], [21] and frequency-division multiple access (FDMA) [11] techniques, or by taking the routing into consideration in a cross-layer framework [22].

The rest of the paper is organized as follows. In Section 2, the related work is discussed. In Section 3, we present the system model. In Section 4, we describe the distributed solution algorithm and in Section 5, we present the globally optimal solution algorithm. In Section 6, we evaluate the proposed algorithm through simulation results and in-field experiments in Lake LaSalle, and finally we draw the main conclusions in Section 7.

2 Related Work

The objective of time scheduling in UW-ASNs is to separate or align multiple interfering signals and hence to avoid

interference [5], [10], [12], [23], [24], [25], [26], [27], [28], [29], [30], [31], [32], [33], [34]. For example, in [5] Syed *et al*. proposed a modified version of a slotted ALOHA protocol by adding a guard band to each transmission slot, and showed that this can considerably improve throughput in UW-ASNs with short communication ranges and with global synchronization. In [25], Kredo *et al*. proposed a staggered TDMA underwater MAC protocol (STUMP), which is a scheduled, collision free TDMA-based MAC protocol that leverages the low propagation speed of the underwater channel and node position diversity. The protocol makes use of the propagation delay information to overlap node communication and increase channel utilization. In [26], Yun and Lim proposed a geometric spatial reuse-TDMA (GSR-TDMA) MAC protocol for centralized, multihop UW-ASNs. The underwater nodes are periodically scheduled after determining their location information. The GSR-TDMA scheme can increase the number of underwater nodes that send packets at the same time. Similarly, in [23] Mandal and De investigated a RSS-ALOHA based slot reservation protocol, with the objective of maximizing the network utilization by considering centralized UW-ASNs with perfect synchronization and propagation delay information from each source node to the common gateway node. In our previous work [12], we implemented and evaluated a hybrid MAC protocol in cluster-based multi-hop UW-ASNs. The protocol relies on TDMA for intra-cluster centralized scheduling and on CSMA/CA for inter-cluster distributed channel access. Different from these MAC protocols, which mostly attempt to mitigate the negative effect of the spatial uncertainty of interference, Chitre *et al*. pointed out in [10] that the large and distance-dependent propagation delay can be exploited through interference alignment (IA) in the time domain to achieve much higher throughput than achievable without spatial uncertainty. This however largely relies on exact knowledge of global location information of all nodes and on centralized control, which is not easy to implement in practice. Similarly, in our previous work [35] on underwater CDMA-based analog network coding, we showed how interference can be leveraged to improve the channel utilization. Pan *et al.* proposed in [27] a MAC protocol based on slotted floor acquisition multiple access (FAMA) for underwater acoustic WiFi networks. In [28], the authors proposed an adaptive MAC protocol for TDMA-based underwater acoustic sensor networks with dynamic traffic, assuming perfect synchronization among the nodes. A collision-free depth-based layering TDMA MAC protocol called DL-MAC is proposed for UWSNs in [29]. Readers are referred to [36], [37] for comprehensive surveys of the main research developments in this field. Different from existing work, which either requires perfect synchronization, signalling exchange among the nodes or centralized coordination, this paper focuses on distributed, asynchronous and light-weight stochastic MAC protocols.

Several of the protocols discussed above also fall within the class of stochastic underwater MAC protocols with a focus on time-domain interference avoidance, e.g., [5], [12], [23], [24]. Additional representative contributions can be found in [12], [20], [38], [39], [40], [41], [42], [43] and references therein. In [20], we proposed a hybrid UW-MAC that jointly exploits the light weight property of ALOHA and the robustness of CDMA for frequency selective fading channels, by considering Rayleigh fading shallow water channel

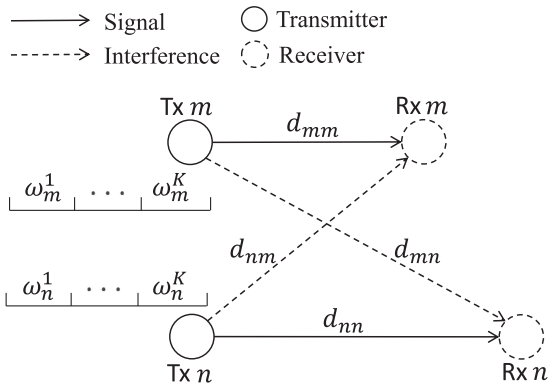

Fig. 1. System model for underwater acoustic sensor networks.

and static multiuser access interference. In [39], Patil *et al.* proposed a stochastic model for the performance evaluation of depth based routing (DBR) protocol. In [40], Han *et al*. proposed a stochastic MAC protocol with randomized power control for UW-ASNs, called SMARP. A randomized power control is implemented based on the propagation loss model of acoustic channels to improve the network throughput. In [41], Rahmati and Pompili proposed a probabilistic MAC based on space division multiple access (SDMA) for short to medium distances that makes use of inherent position uncertainty of the moving vehicles in underwater. In [42], Marinakis *et al*. proposed a stochastic transmission strategy based on the ALOHA protocol. A stochastic scheduling is used where time is slotted, and each network node broadcasts at each time slot according to some probability. A distributed heuristic based on local network density is presented and evaluated using numerical simulations. In [43], Lu *et al*. presented a random access transmission scheme that takes into consideration the physical-layer information of the channel. In [44], Stefanov and Stojanovic analyzed the throughput performance of ALOHA by characterizing the statistical behavior of multiuser access interference with the objective of providing a potential to turn the complex interference uncertainty into an advantage for underwater communications. Sharing the same objective as in [44], in this work, we design an underwater MAC protocol that jointly considers statistical network interference, the asynchronous transmission behavior of each node, and the stochastic nature of random traffic arrivals. We develop a cross-layer optimization framework and accordingly design both distributed and centralized solution algorithms.

3 System Model

We consider an underwater acoustic sensor network consisting of a set $\mathcal{N}$ of parallel sessions that share a given portion of the acoustic spectrum. As shown in Fig. 1, each session $n \in \mathcal{N}$ consists of a source-destination pair, i.e., transmitter n and its intended receiver, denoted as receiver n accordingly. Different sessions do not share the same transmitter or receiver node. The transmission time is divided into consecutive time slots (aka packet slot, as one packet can be transmitted in each slot), which are further organized into consecutive frames each composed of a set $\mathcal{K}$ of time slots with $|\mathcal{K}| = K$. Each transmitter $n \in \mathcal{N}$ decides

its transmission strategy for each time slot in a frame while using the same strategy for all frames. In the kth time slot of each frame, transmitter n either transmits a packet with probability $\omega_n^k \in [0,\ 1]$, or it stays silent with probability $1-\omega_n^k$ and enqueues its incoming packets in its buffer. We denote the transmission probability profile as $\boldsymbol{\omega}_n = (\omega_n^k)_{k\in\mathcal{K}}$ for user $n \in \mathcal{N}$ and $\boldsymbol{\omega} = (\boldsymbol{\omega}_n)_{n\in\mathcal{N}}$ for all users.

Consider finite buffer size for each node, then a packet from user $n \in \mathcal{N}$ may be lost either because of a transmission error or overflow. If we denote the corresponding packet loss rates of user $n \in \mathcal{N}$ as $P_n^{\text{err}}(\boldsymbol{\omega})$ and $P_n^{\text{ofl}}(\boldsymbol{\omega}_n)$, respectively, then the overall packet loss rate of user n denoted as $P_n^{\text{los}}(\boldsymbol{\omega})$ can be represented as

$$P_n^{\text{los}}(\boldsymbol{\omega}) = P_n^{\text{err}}(\boldsymbol{\omega}) + P_n^{\text{ofl}}(\boldsymbol{\omega}_n) - P_n^{\text{err}}(\boldsymbol{\omega})P_n^{\text{ofl}}(\boldsymbol{\omega}_n). \tag{1}$$

Next, we derive an explicit expression for $P_n^{\text{los}}(\boldsymbol{\omega})$ by describing the channel model, interference model and queueing model in sequence.

Channel Model. Denote h_{mn} as the channel gain from transmitter m to receiver n. Then, h_{mn} can be represented as

$$h_{mn} = H_{mn}\rho^2, \tag{2}$$

where ρ represents the fading coefficient[2], and H_{mn} represents the transmission loss that a narrow-band-acoustic signal experiences over a given spectrum and can be described by the Urick propagation model as [45]

$$H_{mn} = d_{mn}^{-2} \cdot 10^{-\frac{a\cdot d_{mn}+A_{mn}}{10}}, \tag{3}$$

where a [dB/m] represents the medium absorption coefficient, A_{mn} [dB] is the transmission anomaly accounting for degradation of the acoustic intensity caused by multiple path propagation, refraction, diffraction, and scattering of sound [46], [47], [48], [49], [50], and d_{mn} [m] represents the distance between the mth transmitter to the nth receiver.[3]

The channel model in (2) is applicable to both shallow and deep water environments. We focus on the former case, where the acoustic channel is more affected by multipath. We therefore assume that the number of rays goes to infinity and therefore consider a *worst-case scenario*; then, we have $A_{mn} \in [5,\ 10]$ for $m, n \in \mathcal{N}$ [46], [47] and the fading coefficient ρ can be modeled using a unit-mean Rayleigh distributed random variable with cumulative distribution function expressed as

$$\mathrm{P}[\rho \le x] = 1 - \exp\left(-\frac{\pi x^2}{4}\right). \tag{4}$$

2. The fading coefficient is a function of time. We omit the dependence on time to avoid confusion with the slotted structure of the frame. Moreover, we assume the fading coefficients in different time slots to be independent of each other, while the time correlation of fading coefficients will be studied in future work.

3. In (3) we consider spherical spreading model as an example. However, it is worth pointing out that the stochastic channel access scheme proposed in this work does not depend on any specific spreading loss model. Since we focus on characterizing the aggregate interference of multiple randomly deployed nodes in underwater acoustic networks, both the resulting communication range and spreading loss are random. We propose to fit the shaping parameters of Gamma distribution function based on the first- and second-order moment information of the aggregate interference and validate the effectiveness of this approach using testbed experiments.

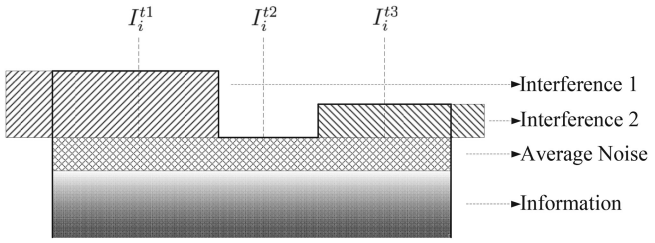

Fig. 2. The received signal is sampled at three points during a time slot. The signal at each sampling point consists of information signal, noise and interfering signal. Information signal and noise keep the same for different sampling points.

The proposed distributed channel access scheme can also be extended to the deep water case, where the acoustic channel is less severely affected by multipath with $A_{m,n} \in [0,\ 5]$, $m, n \in \mathcal{N}$ and $\rho = 1$.

Interference Model. Because of the distance-dependent propagation delay, acoustic signals transmitted simultaneously by different devices in general do not arrive at an intended receiver at the same time. As a result, the interference observed at a receiver and hence its transmission behavior is nontrivially coupled with the transmission strategy $\boldsymbol{\omega}$, which makes interference modeling rather challenging. To the best of our knowledge, in the existing literature there is no interference model that can characterize the statistical behavior of interference in multiuser underwater networks.

We consider an L-measurement interference model, in which each receiver $n \in \mathcal{N}$ measures the received signal at a set $\mathcal{L}_n^k$ of time instants during the kth time slot of each frame.[4] Then, the measured interference can be represented as a vector, denoted as $\mathcal{I}_n^k = (I_n^{kl})_{l\in\mathcal{L}_n^k}$, where I_n^{kl} represents the lth interference measurement. Fig. 2 shows an example of the L-measurement method with $L = 3$. Denote g_{mn}^{kl}, with $l \in \mathcal{L}_n^t$, as the time slot in which user $m \in \mathcal{N} \setminus n$ causes interference to user n at the lth measurement point of the kth time slot in each frame. Then, the measured interference power can be expressed as

$$I_n^{kl}(\boldsymbol{\omega}) = \sum_{m\in\mathcal{N}\setminus n} P_m h_{mn}\alpha(g_{mn}^{kl}), \tag{5}$$

where P_m [W] represents the transmission power of transmitter m, and the indicator function $\alpha(g_{mn}^{kl}) = 1$ if transmitter m sent a packet that is received by receiver n at lth interference sample of kth time slot, i.e., transmitter n sent a packet at (g_{mn}^{kl})th time slot, and $\alpha(g_{mn}^{kl}) = 0$ otherwise.

In this work, we use as in [51], [52] a Gamma distribution function $\gamma_n^{kl}(x,\ \boldsymbol{\omega})$ to characterize the probability density function (pdf) of I_n^{kl} defined in (5). Then we have,

$$\mathrm{pdf}[I_n^{kl} = x] = \gamma_n^{kl}(x,\ \boldsymbol{\omega}) = \frac{x^{\eta_n^{kl}(\boldsymbol{\omega})-1}e^{-x/\theta_n^{kl}(\boldsymbol{\omega})}}{\Gamma\left(\eta_n^{kl}(\boldsymbol{\omega})\right)\left(\theta_n^{kl}(\boldsymbol{\omega})\right)^{\eta_n^{kl}(\boldsymbol{\omega})}}, \tag{6}$$

where $\eta_n^{kl}(\boldsymbol{\omega})$ and $\theta_n^{kl}(\boldsymbol{\omega})$ are shaping parameters that can be estimated online as explained later in Section 4, and gamma

4. The optimal number of measurements during a time slot needs to be determined through off-line measurement or can be estimated through online learning techniques. We assume that the number of measurements is known.

function $\Gamma\big(\eta_n^{kl}(\boldsymbol{\omega})\big) = \int_0^\infty x^{\eta_n^{kl}(\boldsymbol{\omega})-1}e^{-x}dx$. Later in Section 6, we will validate the interference model based on testbed channel measurements using Teledyne Benthos Telesonar SM-75 underwater modems [53] - extensive experimental results show that the model captures the statistical characteristics of interference very accurately. Then, the cumulative distribution function (cdf) of I_n^{kl}, denoted as $\vartheta_n^{kl}(x,\ \boldsymbol{\omega})$, can be represented as

$$\mathrm{P}[I_n^{kl} \le x] = \vartheta_n^{kl}(x,\boldsymbol{\omega}) = \frac{\varphi\big(\eta_n^{kl}(\boldsymbol{\omega}), \frac{x}{\theta_n^{kl}(\boldsymbol{\omega})}\big)}{\Gamma\big(\eta_n^{kl}(\boldsymbol{\omega})\big)}, \tag{7}$$

where $\varphi\big(\eta_n^{kl}(\boldsymbol{\omega}), \frac{x}{\theta_n^{kl}(\boldsymbol{\omega})}\big) = \int_0^{\frac{x}{\theta_n^{kl}(\boldsymbol{\omega})}} s^{\eta_n^{kl}(\boldsymbol{\omega})-1}e^{-s}ds$ is the lower incomplete gamma function.

If we let SINR_n^{kl} represent the signal-to-interference-plus-noise ratio (SINR) at receiver $n \in \mathcal{N}$ at the lth measurement point in the kth time slot of each frame, then SINR_n^{kl} can be expressed as

$$\mathrm{SINR}_n^{kl}(\boldsymbol{\omega}) = \frac{P_n h_{nn}}{I_n^{kl}(\boldsymbol{\omega}) + \delta_n^2}, \tag{8}$$

where δ_n^2 represents the noise power at receiver $n \in \mathcal{N}$. For given transmission strategies, i.e., transmission rate R_n^0, modulation and coding schemes, a one-to-one mapping between the resulting bit error rate (BER) before decoding denoted as BER_n^{kl} and the transmission rate can be established as [54]

$$R_n^0 = \log\left(1 + K_n^{kl}\mathrm{SINR}_n^{kl}(\boldsymbol{\omega})\right) \tag{9}$$

where

$$K_n^{kl} = \frac{-\phi_{n,1}}{\log\left(\phi_{n,2}\mathrm{BER}_n^{kl}(\boldsymbol{\omega})\right)}, \tag{10}$$

in which $\phi_{n,1}$ and $\phi_{n,2}$ are parameters depending on the modulation schemes used by session n. Then, we have

$$\mathrm{BER}_n^{kl}(\boldsymbol{\omega}) = \frac{e^{\frac{-\phi_{n,1}\mathrm{SINR}_n^{kl}(\boldsymbol{\omega})}{e^{R_n^0}-1}}}{\phi_{n,2}}, \tag{11}$$

and the average BER of time slot k denoted as $\mathrm{BER}_n^k(\boldsymbol{\omega})$ can be expressed as

$$\mathrm{BER}_n^k(\boldsymbol{\omega}) = \frac{1}{L}\sum_{l=1}^{L}\mathrm{BER}_n^{kl}(\boldsymbol{\omega}). \tag{12}$$

For a given channel coding scheme, denote $\mathrm{BER}_{\mathrm{th}}$ the maximum BER that a packet can successfully be decoded, and $\beta_n^k(\boldsymbol{\omega})$ represent the packet decoding success probability that occurs when $\mathrm{BER}_n^k \le \mathrm{BER}_{\mathrm{th}}$. Then, $\beta_n^k(\boldsymbol{\omega})$ can be expressed as

$$\begin{aligned}\beta_n^k(\boldsymbol{\omega}) &\triangleq \mathrm{P}(\mathrm{BER}_n^k \le \mathrm{BER}_{\mathrm{th}})\\ &= \int_0^{\mathrm{BER}_{\mathrm{th}}} \beta_n^{k1}(x_1)\int_{x_1}^{\mathrm{BER}_{\mathrm{th}}}\beta_n^{k2}(x_2)\cdots\\ &\quad \int_{\sum_{l=1}^{L-1}x_l}^{\mathrm{BER}_{\mathrm{th}}}\beta_n^{kL}(x_L)\,\mathrm{d}x_1\mathrm{d}x_2\cdots\mathrm{d}x_L\end{aligned} \tag{13}$$

where $\beta_n^{kl}(x_l)$ is the pdf of BER at the lth measurement point in kth time slot of each frame, and for each $1 \le l \le L$ can be calculated as,

$$\beta_n^{kl}(x_l) = \gamma_n^{kl}(\mathrm{SINR}_n^{kl},\ \boldsymbol{\omega}), \tag{14}$$

with

$$\mathrm{SINR}_n^{kl} = \frac{\log\left(x_l\phi_{n,2}\right)e^{R_n^0}-1}{-\phi_{n,1}}. \tag{15}$$

Then, the overall packet error rate of user n caused by transmission errors, i.e., $P_n^{\mathrm{err}}(\boldsymbol{\omega})$ in (1), can be written as

$$P_n^{\mathrm{err}}(\boldsymbol{\omega}) = \frac{1}{\sum_{k\in\mathcal{K}}\omega_n^k}\sum_{k\in\mathcal{K}}\omega_n^k(1-\beta_n^k(\boldsymbol{\omega})), \tag{16}$$

where $\beta_n^k(\boldsymbol{\omega})$ is defined in (13).

Queueing Model. Consider a queue with finite buffer size of $Q_{\max}$ packets for each node. Whenever the queue length reaches the maximum $Q_{\max}$, newly incoming packets will be dropped directly. The packet drop rate P_n^{ofl} for session $n \in \mathcal{N}$ depends on the packet incoming process and the packet service process.

We first define the packet service process for session n based on the transmission profile $\boldsymbol{\omega}_n$. Let random variable ν_n represent the number of consecutive time slots it takes for user $n \in \mathcal{N}$ to transmit a packet. Then, the pdf of ν_n can be expressed as

$$\mathrm{P}[\nu_n = z] = \begin{cases}\frac{1}{K}\sum_{k\in\mathcal{K}}\omega_n^k, & z = 1,\\ \frac{1}{K}\sum_{k\in\mathcal{K}}\prod_{g\in\mathcal{K}_k}(1-\omega_n^g)\omega_n^k, & 1 < z \le K,\\ \left(\prod_{k\in\mathcal{K}}(1-\omega_n^k)\right)^{\hat{z}}\mathrm{P}[\nu_n = \tilde{z}], & z > K,\end{cases} \tag{17}$$

where $\hat{z} = \left\lfloor\frac{z}{K}\right\rfloor$, $\tilde{z} = z - K\cdot\hat{z}$, and ω_n^g represents the transmission probability of the gth time slot in a frame with $\mathcal{K}_k$ representing the set of indices of the $z-1$ consecutive time slots before the kth time slot; for example, if $z = 3$ and each frame consists of at least three time slots, i.e., $K \ge 3$, then we have $\mathcal{K}_k = \{K-1,\ K-2\}$ for $k = K$, and $\mathcal{K}_k = \{K,\ K-1\}$ for $k = 1$.

We observe from (17) that, the expression of $\mathrm{P}[\nu_n = z]$ is a complex function of the transmission profile $\boldsymbol{\omega}_n$. To facilitate theoretical tractability, we approximate $\mathrm{P}[\nu_n = z]$ in (17) through an exponential distribution function

$$\widetilde{\mathrm{P}}[\nu_n = z] = \phi(\boldsymbol{\omega}_n)e^{-\phi(\boldsymbol{\omega}_n)z},\ \forall n \in \mathcal{N}, \tag{18}$$

where the service rate parameter $\phi(\boldsymbol{\omega}_n)$, which only depends on $\boldsymbol{\omega}_n$ (the transmission probability profile of user n), is set to the average service rate in a frame according to (17), i.e., $\phi(\boldsymbol{\omega}_n) = \frac{1}{K}\sum_{k\in\mathcal{K}}\omega_n^k$.

We assume that the incoming packets generated at each user $n \in \mathcal{N}$ follow a Poisson arrival process with average packet arrival rate λ_n [packets/sec]. Then, the queue of each user $n \in \mathcal{N}$ can be modeled using a truncated $M/M/1$ queue with buffer size of $Q_{\max}$ packets, and the packet drop rate of user n due to overflow can be represented as [55, chap. 2] as follows:

$$P_n^{\mathrm{ofl}}(\boldsymbol{\omega}_n) = \begin{cases}\frac{1-\frac{\lambda_n}{\sum_{k\in\mathcal{K}}\omega_n^k}}{1-\left(\frac{\lambda_n}{\sum_{k\in\mathcal{K}}\omega_n^k}\right)^{Q_{\max}+1}}\left(\frac{\lambda_n}{\sum_{k\in\mathcal{K}}\omega_n^k}\right)^{Q_{\max}}, & \text{if } \lambda_n \ne \sum_{k\in\mathcal{K}}\omega_n^k,\\ \frac{1}{Q_{max}+1}, & \text{otherwise.}\end{cases} \tag{19}$$

Expected Throughput. Based on above formulations and according to (1), the expected packet throughput of user $n \in \mathcal{N}$, denoted as $R_n(\boldsymbol{\omega})$, can be expressed as

$$R_n(\boldsymbol{\omega}) = \lambda_n\big(1 - P_n^{\text{ofl}}(\boldsymbol{\omega}_n) - P_n^{\text{err}}(\boldsymbol{\omega}) + P_n^{\text{ofl}}(\boldsymbol{\omega}_n)P_n^{\text{err}}(\boldsymbol{\omega})\big), \tag{20}$$

and can be rewritten approximately by neglecting the second-order term $P_n^{\text{ofl}}(\boldsymbol{\omega}_n)P_n^{\text{err}}(\boldsymbol{\omega})$ as

$$R_n(\boldsymbol{\omega}) = \lambda_n\big(1 - P_n^{\text{ofl}}(\boldsymbol{\omega}_n) - P_n^{\text{err}}(\boldsymbol{\omega})\big). \tag{21}$$

Then, the ideal objective of our problem would be to maximize the sum throughput of all users in $\mathcal{N}$ under certain predefined fairness criterion, by adjusting the transmission strategy $\boldsymbol{\omega}_n$ of each user $n \in \mathcal{N}$, i.e.,

$$\begin{aligned} \text{Given}: \quad & P,\ d_{mn},\ N_n,\ \forall m, n \in \mathcal{N} \\ \underset{\boldsymbol{\omega}}{\text{maximize}}: \quad & U(\boldsymbol{\omega}) = \sum_{n\in\mathcal{N}} \log R_n(\boldsymbol{\omega}) \\ \text{subject to}: \quad & 0 \le \omega_n^k \le 1,\ \forall k \in \mathcal{K},\ \forall n \in \mathcal{N}, \end{aligned} \tag{22}$$

where the logarithm operation is introduced to achieve proportional fairness among the users.

However, this objective is clearly not achievable with distributed control. Furthermore, the centralized optimization problem is not convex, which means that, in general, only suboptimal solutions can be computed in polynomial time even with centralized algorithms. With this understanding, we first propose a low-complexity distributed solution algorithm, and then present a centralized algorithm to compute the globally optimal solution to provide a benchmark for the performance of the proposed distributed algorithm.

4 Distributed Algorithm Design

Based on the system model developed in Section 3, we now present a distributed problem formulation and a low-complexity distributed algorithm. Then, we discuss several issues related to the implementation of the algorithm. The distributed solution algorithm is designed based on a best-response strategy, i.e., each node iteratively and asynchronously solves the problem of dynamic queueing and transmission in UW-ASNs. At each iteration, each user individually maximizes its own expected throughput based on the statistical characterization of the interference obtained through past observations and based on its queue information.

We let $\boldsymbol{\omega}_{-n} = (\boldsymbol{\omega}_m)_{m\in\mathcal{N}\setminus n}$ represent the transmission probability profile of all users in $\mathcal{N}$ except n. Then, the expected throughput $R_n(\boldsymbol{\omega})$ in (21) can be equivalently expressed as $R_n(\boldsymbol{\omega}_n, \boldsymbol{\omega}_{-n})$, i.e.,

$$R_n(\boldsymbol{\omega}_n, \boldsymbol{\omega}_{-n}) = \lambda_n\big(1 - P_n^{\text{ofl}}(\boldsymbol{\omega}_n) - P_n^{\text{err}}(\boldsymbol{\omega}_n, \boldsymbol{\omega}_{-n})\big), \tag{23}$$

where $P_n^{\text{err}}(\boldsymbol{\omega}_n, \boldsymbol{\omega}_{-n})$ is the corresponding equivalent representation of $P_n^{\text{err}}(\boldsymbol{\omega})$ given in (16). Then, at each iteration, each user $n \in \mathcal{N}$ optimally chooses its transmission probability vector $\boldsymbol{\omega}_n$ by solving the following optimization problem,

$$\begin{aligned} \text{Given}: \quad & P_n,\ d_{nn}, \delta_n^2,\ \lambda_n, \\ & \eta_n^{kl}(\boldsymbol{\omega}_{-n}),\ \theta_n^{kl}(\boldsymbol{\omega}_{-n}),\ \forall k \in \mathcal{K},\ \forall l \in \mathcal{L}_n^k \\ \underset{\boldsymbol{\omega}_n}{\text{maximize}}: \quad & R_n(\boldsymbol{\omega}_n,\ \boldsymbol{\omega}_{-n}) \\ \text{subject to}: \quad & 0 \le \omega_n^k \le 1,\ \forall k \in \mathcal{K} \end{aligned} \tag{24}$$

where d_{nn} represents the distance between transmitter n and receiver n, δ_n^2 is the noise power at receiver n, the objective function $R_n(\boldsymbol{\omega}_n, \boldsymbol{\omega}_{-n})$ is defined through (16) and (19), $\eta_n^{kl}(\boldsymbol{\omega}_{-n})$ and $\theta_n^{kl}(\boldsymbol{\omega}_{-n})$ are the shaping parameters in (6) depending on the transmission strategies of all other users in $\mathcal{N} \setminus n$, i.e., $\boldsymbol{\omega}_{-n}$.

Individual Optimization. It is nontrivial for each user $n \in \mathcal{N}$ to determine its own optimal transmission strategy $\boldsymbol{\omega}_n$, because the above optimization problem is in general nonlinear and non-convex due to non-convexity of the expression in (16). In the following, we propose an efficient algorithm to search for the globally optimal solution by taking advantage of the special structure of the objective function $R_n(\boldsymbol{\omega}_n,\ \boldsymbol{\omega}_{-n})$.

To maximize $R_n(\boldsymbol{\omega}_n,\ \boldsymbol{\omega}_{-n})$ in (24), each user $n \in \mathcal{N}$ only needs to minimize its overall packet loss rate

$$P_n^{\text{los}}(\boldsymbol{\omega}) = P_n^{\text{err}}(\boldsymbol{\omega}_n, \boldsymbol{\omega}_{-n}) + P_n^{\text{ofl}}(\boldsymbol{\omega}_n), \tag{25}$$

where $P_n^{\text{err}}(\boldsymbol{\omega}_n, \boldsymbol{\omega}_{-n})$ and $P_n^{\text{ofl}}(\boldsymbol{\omega}_n)$ are defined in (16) and (19), respectively. To this end, we introduce a new intermediate variable $y_n \triangleq \sum_{k\in\mathcal{K}} \omega_n^k$. Then, with given y_n, $P_n^{\text{los}}(\boldsymbol{\omega})$ in (25) can be minimized over $\boldsymbol{\omega}_n$ by solving a linear optimization problem. Denote the resulting minimum as $\min_{\boldsymbol{\omega}_n} P_n^{\text{los}}(y_n, \boldsymbol{\omega}_{-n}, \boldsymbol{\omega}_n)$. Then, the optimization problem formulated in (24) can be equivalently expressed as, for each $n \in \mathcal{N}$,

$$\begin{aligned} \text{Given}: \quad & P_n,\ d_{nn},\ N_n,\ \lambda_n, \\ & \eta_n^{kl}(\boldsymbol{\omega}_{-n}),\ \theta_n^{kl}(\boldsymbol{\omega}_{-n}),\ \forall k \in \mathcal{K},\ \forall l \in \mathcal{L}_n^k \\ \underset{y_n}{\text{minimize}}: \quad & \min\nolimits_{\boldsymbol{\omega}_n} P_n^{\text{los}}(y_n, \boldsymbol{\omega}_{-n}, \boldsymbol{\omega}_n) \\ \text{subject to}: \quad & y_n \ge 0 \\ & y_n \le K \\ & 0 \le \omega_n^k \le 1,\ \forall k \in \mathcal{K} \\ & \sum_{k\in\mathcal{K}} \omega_n^k \ge y_n. \end{aligned} \tag{26}$$

We found experimentally that the objective function in (26), i.e., $\min_{\boldsymbol{\omega}_n} P_n^{\text{los}}(y_n, \boldsymbol{\omega}_{-n}, \boldsymbol{\omega}_n)$, is a quasi-convex function of y_n [56, Section 3.4] for a wide set of network settings. An example verification of the quasi-convexity is shown in Fig. 3. This implies that the globally optimal solution of y_n can be iteratively calculated in logarithmic time (which is less than polynomial) by using the bisection method. At each iteration, the optimal transmission probability vector $\boldsymbol{\omega}_n$ for a given y_n can be obtained by simply solving a linear optimization problem. The proposed distributed solution algorithm is summarized in Algorithm 1, and the overall diagram of the stochastic channel access scheme is illustrated in Fig. 4. It is worth pointing out that the optimization algorithm causes only low communication overhead because there is no need to update the transmission probability profile frequently, e.g., it may be enough to send an update once every 100 frames to adapt to the dynamic

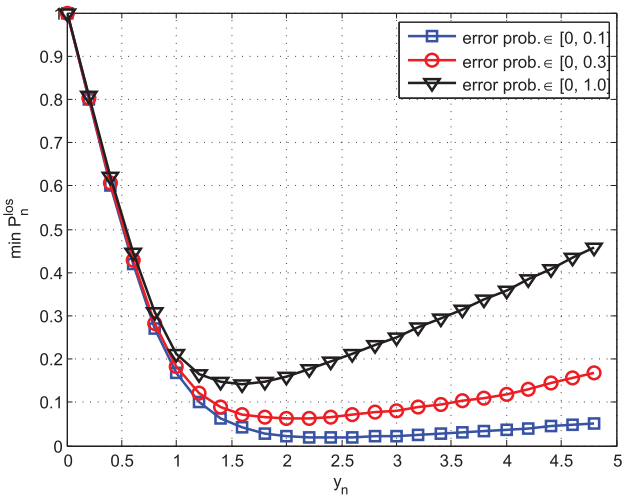

Fig. 3. Example verification of quasi-convexity of the objective function in (26).

interference environment, which accounts for all the interfering transmission activities during each update period.

Algorithm 1. Distributed Solution Algorithm

Data Input: $P_n,\ d_{nn},\ N_n$, for all $n \in \mathcal{N}$, $\nu_{\max}, \kappa = 0.01$
1 **Initialize**: Set $\nu = 0$, $\boldsymbol{\omega}_n(\nu) = \boldsymbol{\omega}_n^0,\ \forall n \in \mathcal{N}$
2 **while** $||\boldsymbol{\omega}_n(\nu) - \boldsymbol{\omega}_n(\nu-1)|| > \kappa,\ \forall n \in \mathcal{N}$ or $\nu < \nu_{\max}$ **do**
3 Each user $n \in \mathcal{N}$ finds $\boldsymbol{\omega}_n^*$ to minimize $P_n^{\text{los}}(y_n, \boldsymbol{\omega}_{-n}, \boldsymbol{\omega}_n)$ by searching for the optimal y_n through solving the optimization problem in (26).
4 Set $\boldsymbol{\omega}_n(\nu) = \boldsymbol{\omega}_n^*$ for each $n \in \mathcal{N}$.
5 Set $\nu \leftarrow \nu + 1$.
6 **end**

Implementation Issues. In the proposed distributed access scheme, each node $n \in \mathcal{N}$ individually maximizes its own throughput for a given transmission strategy of the interfering users $\boldsymbol{\omega}_{-n}$. However, in a fully distributed algorithm, $\boldsymbol{\omega}_{-n}$ is in general unavailable to user n. A nice property of our proposed algorithm is that for practical implementation each user n only needs to estimate the two shaping parameters $\eta_n^{kl}(\boldsymbol{\omega}_{-n})$ and $\theta_n^{kl}(\boldsymbol{\omega}_{-n})$ of the interference probability distribution based on the past observations of interference at the receiver side.

For this purpose, let $\mathrm{E}[I_n^{kl}]$ and $\mathrm{D}[I_n^{kl}]$ represent mean and variance of I_n^{kl}, respectively. Then, we can derive them as

$$\begin{aligned}\mathrm{E}[I_n^{kl}] &= \mathrm{E}\Big[\sum_{m\in\mathcal{N}\setminus n} P_m h_{nm}\alpha(g_{nm}^{kl})\Big] \\ &= \sum_{m\in\mathcal{N}\setminus n} P_m \omega_m^{g_{nm}^{kl}} H_{nm}\mathrm{E}[\rho^2],\end{aligned} \tag{27}$$

$$\begin{aligned}\mathrm{D}[I_n^{kl}] &= \mathrm{D}\Big[\sum_{m\in\mathcal{N}\setminus n} P_m h_{nm}\alpha(g_{nm}^{kl})\Big] \\ &= \sum_{m\in\mathcal{N}\setminus n} P_m^2 \omega_m^{g_{nm}^{kl}} (H_{nm})^2\mathrm{D}[\rho^2],\end{aligned} \tag{28}$$

where $\mathrm{E}[\rho^2] = \frac{4}{\pi}$ and $\mathrm{D}[\rho^2] = \frac{16}{\pi^2}$ according to (4).

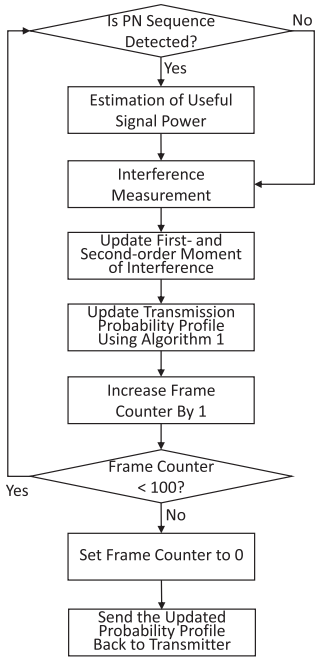

Fig. 4. Diagram of the stochastic channel access scheme.

According to the probability density function of the interference I_n^{kl} in (6), $\mathrm{E}[I_n^{kl}]$ and $\mathrm{D}[I_n^{kl}]$ can also be represented as

$$\mathrm{E}[I_n^{kl}] = \eta_n^{kl}(\boldsymbol{\omega})\theta_n^{kl}(\boldsymbol{\omega}), \tag{29}$$

$$\mathrm{D}[I_n^{kl}] = \eta_n^{kl}(\boldsymbol{\omega})[\theta_n^{kl}(\boldsymbol{\omega})]^2, \tag{30}$$

where $\eta_n^{kl}(\boldsymbol{\omega})$ and $\theta_n^{kl}(\boldsymbol{\omega})$ are the two shaping parameters in (6). Then, from (27), (28), 29, and (30), we have

$$\theta_n^{kl}(\boldsymbol{\omega}) = \mathrm{D}[I_n^{kl}]/\mathrm{E}[I_n^{kl}], \tag{31}$$

$$\eta_n^{kl}(\boldsymbol{\omega}) = (\mathrm{E}[I_n^{kl}])^2/\mathrm{D}[I_n^{kl}], \tag{32}$$

where $\mathrm{E}[I_n^{kl}]$ and $\mathrm{D}[I_n^{kl}]$ are given in (27), (28), respectively.

Therefore, it is sufficient for each user to fully characterize the statistical behavior of interference at its receiver, by recording the observed interference levels and then calculating the mean and variance. In case of variations in the network topology, e.g., when nodes join or leave the network, $\eta_n^{kl}(\boldsymbol{\omega})$ and $\theta_n^{kl}(\boldsymbol{\omega})$ need to be re-estimated, which might trigger another round of transmission probability adaptation. To measure the mean in (27) and variance in (28), as illustrated in Fig. 4, each receiver node can first estimate the power of the received useful signal and then subtract it from that of the overall signal. Given the transmission power of the transmitter, this can be accomplished by letting the transmitter send a predefined PN sequence. The receiver can then estimate the channel state information (CSI) through PN sequence cross-correlation.

5 Centralized Solution Algorithm

As discussed in Section 3, an ideal objective would be to maximize the sum throughput of all users in the network. The objective can not be achieved trivially due to lack of

centralized control and non-concavity of the utility function $R_i(\boldsymbol{\omega}_i, \boldsymbol{\omega}_{-i})$ in (21). In this section, we develop a centralized but globally optimal solution algorithm based on the *combination of branch and bound framework [57], [58] and convex relaxation techniques [59]* to solve the social optimization problem in (22).

Algorithm Overview. The proposed algorithm searches for a globally optimal solution that satisfies the predefined precision of optimality $\varepsilon \in (0, 1)$. Denote the global optimum of the objective function in (22) as R^*, then the algorithm iteratively searches for an ε-optimal solution R such that $R \geq \varepsilon R^*$. The optimality precision ε can be set as close to 1 as we wish, at the cost of higher computational complexity for larger ε. For this purpose, the algorithm maintains a global upper bound $\mathrm{UP}_{\mathrm{glb}}$ and a global lower bound $\mathrm{LR}_{\mathrm{glb}}$ on sum-throughput R in (22), then it must be

$$\mathrm{LR}_{\mathrm{glb}} \leq R^* \leq \mathrm{UP}_{\mathrm{glb}}. \tag{33}$$

We use $\mathrm{UP}_{\mathrm{glb}}$ and $\mathrm{LR}_{\mathrm{glb}}$ to drive the branch and bound iteration, and to check how close the obtained solution is to R^* and decide when to terminate the iteration. If $\mathrm{LR}_{\mathrm{glb}} \geq \varepsilon \mathrm{UP}_{\mathrm{glb}}$, the algorithm terminates and sets the optimal objective value to $R = \mathrm{LR}_{\mathrm{glb}}$.

The algorithm also maintains a set of sub-domains $\boldsymbol{\Omega} = \{\boldsymbol{\Omega}_\nu \subseteq \boldsymbol{\Omega}_0,\ \nu = 1, 2, \ldots\}$, with $\boldsymbol{\Omega}_0 = \{\boldsymbol{\omega}\}$ being the initial domain that includes all possible $\boldsymbol{\omega} = (\boldsymbol{\omega}_n)_{n\in\mathcal{N}}$, and ν representing the iteration index. At the beginning of iterations, there is only one element in $\boldsymbol{\Omega}$, i.e., $\boldsymbol{\Omega}_0$. In each iteration, the algorithm selects a sub-domain $\boldsymbol{\Omega}_{\nu^*}$ from $\boldsymbol{\Omega}$ and partitions it into two smaller ones through *domain partition* (as discussed later), say $\boldsymbol{\Omega}^1_{\nu^*}$ and $\boldsymbol{\Omega}^2_{\nu^*}$. For each of them, the algorithm calculates a local upper bound $\mathrm{UP}(\boldsymbol{\Omega}^i_{\nu^*})$ and local lower bound $\mathrm{LR}(\boldsymbol{\Omega}^i_{\nu^*})$ on sum-throughput R over the sub-domain, with $\nu = 1, 2$, by relaxing the associated subproblem to be convex (as discussed later). Then, if $\mathrm{UP}(\boldsymbol{\Omega}^i_{\nu^*}) < \mathrm{LR}_{\mathrm{glb}}$, it implies that it is impossible for the global optimal solution to be located in $\boldsymbol{\Omega}^i_{\nu^*}$, and hence the associated subproblem will not be considered any more in the following iterations. Otherwise, the domain set $\boldsymbol{\Omega}$ is updated as $\boldsymbol{\Omega} \leftarrow \boldsymbol{\Omega} \cup \boldsymbol{\Omega}^n_{\nu^*}$, and the global lower and upper bounds can then be updated as

$$\mathrm{UP}_{\mathrm{glb}} = \max_{\boldsymbol{\Omega}_\nu \in \boldsymbol{\Omega}} \mathrm{UP}(\boldsymbol{\Omega}_\nu), \tag{34}$$

$$\mathrm{LR}_{\mathrm{glb}} = \max_{\boldsymbol{\Omega}_\nu \in \boldsymbol{\Omega}} \mathrm{LR}(\boldsymbol{\Omega}_\nu). \tag{35}$$

As the problem partition progresses, the gap between $\mathrm{UP}_{\mathrm{glb}}$ and $\mathrm{LR}_{\mathrm{glb}}$ converges to 0, and from (33), they converge to the globally maximal sum-throughput R^*. An example illustration of the algorithm is shown in Fig. 5, where the global upper bound $\mathrm{UP}_{\mathrm{glb}}$ is updated from $\mathrm{UP}(\boldsymbol{\Omega}_0)$ to $\mathrm{UP}(\boldsymbol{\Omega}_1)$, and the global lower bound $\mathrm{LR}_{\mathrm{glb}}$ is updated from $\mathrm{LR}(\boldsymbol{\Omega}_0)$ to $\mathrm{LR}(\boldsymbol{\Omega}_2)$, and as a result, the two global bounds get closer to the global optimum R^*.

Convex Relaxation. To relax the objective function in (22) to be convex, we only need to relax the individual utility function of each user. It can be proven that, $P^{\mathrm{dly}}_n(\boldsymbol{\omega})$ defined in (21), i.e., the packet loss rate due to exceeding the maximum delay, is a convex function of $\boldsymbol{\omega}$. The proof is based on the fact that the second derivative of $P^{\mathrm{dly}}_n(\boldsymbol{\omega})$ with respect to $\boldsymbol{\omega}$ is positive, and on the property that affine mapping preserves convexity of functions [56, Section 3.2.2]. Then, we only need to relax the transmission error probability $P^{\mathrm{err}}_n(\boldsymbol{\omega})$ defined in (21) to be convex.

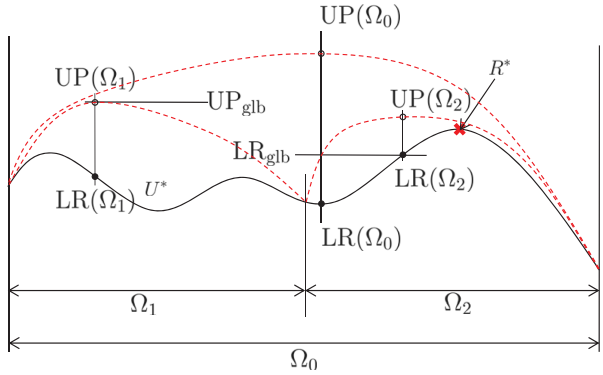

Fig. 5. Example illustration of the solution algorithm.

This can be done in different ways, and users are referred to [59] for details of possible relaxation techniques. In this work, we adopt a simple but effective relaxation method based on the observation that $P^{\mathrm{err}}_n(\boldsymbol{\omega})$ monotonically decreases with transmission probability profile of other sessions $\boldsymbol{\omega}_{-n}$. Denote the current domain of the tth transmission probability variable ω^k_m of $\boldsymbol{\omega}_m$ as $[(\omega^k_m)^{\mathrm{L}}, (\omega^k_m)^{\mathrm{U}}]$. Then, based on the above observation, $P^{\mathrm{err}}_n(\boldsymbol{\omega})$ can be relaxed to $P^{\mathrm{err}}_n(\boldsymbol{\omega}_n, \boldsymbol{\omega}^{\mathrm{U}}_{-n})$ with $\boldsymbol{\omega}^{\mathrm{U}}_{-n} = ((\omega^k_m)^{\mathrm{U}})_{m\in\mathcal{N}\setminus n, k\in\mathcal{K}}$, and finally we obtain a relaxation of $R_n(\boldsymbol{\omega})$ that provides an upper bound on the individual objective function in (22), as illustrated by the red dash line in Fig. 5. Based on the solution obtained through solving the relaxed social optimization problem, we are able to obtain a lower-bound sum throughput using the unrelaxed objective function (22). The two local bounds are then used to update the global upper and lower bounds as in (34) and (35), respectively.

Variable Partition. We select the subproblem that corresponds to the highest local upper bound, and partition it into two new subproblems by partitioning the associated transmission probability variables. In favor of faster convergence, hence lower computational complexity, we consider the effects of variable partition on the level of mutual interference among concurrent sessions. That is, if a session causes only very little interference to the others, the corresponding transmission probability variables will be selected for partition with lower priority, and vice versa. For this purpose, we use the average distance from the source node of a session to the receiver nodes of the other sessions as an indicator, i.e., the smaller the distance, the lower the average interference. Then, by jointly considering the current range of variables, we select $\omega^{k^*}_{n^*}$ for partition such that

$$(n^*, k^*) = \arg\max_{n\in\mathcal{N}, k\in\mathcal{K}} \left((\omega^k_n)^{\mathrm{U}} - (\omega^k_n)^{\mathrm{L}}\right) \frac{1}{dist(n)}, \tag{36}$$

where $dist(n)$ represents the average distance between source node n and the receivers of other sessions. Finally, by partitioning $\omega^{k^*}_{n^*}$ from the middle, i.e., $(\omega^{k^*}_{n^*})^{\mathrm{M}} = \frac{(\omega^{k^*}_{n^*})^{\mathrm{U}} + (\omega^{k^*}_{n^*})^{\mathrm{L}}}{2}$, we obtain two new subproblems corresponding to $[(\omega^{k^*}_{n^*})^{\mathrm{L}}, (\omega^{k^*}_{n^*})^{\mathrm{M}}]$ and $[(\omega^{k^*}_{n^*})^{\mathrm{M}}, (\omega^{k^*}_{n^*})^{\mathrm{U}}]$, respectively.

6 Performance Evaluation

We first experimentally verify the effectiveness of the channel model, interference model and the queueing model

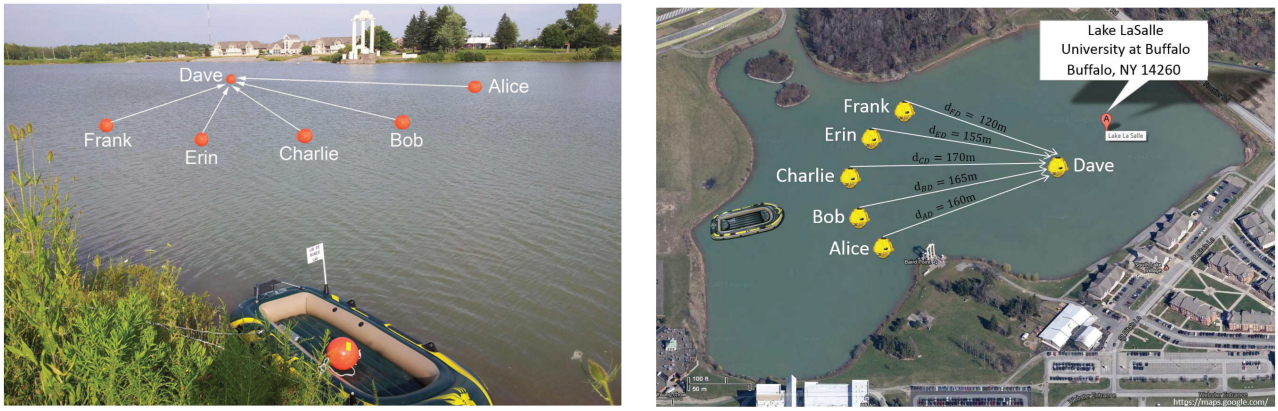

(a) (b)

Fig. 6. (a) Deployment of the six underwater acoustic modems in Lake LaSalle at the University at Buffalo; (b) Aerial view of the underwater acoustic testbed.

adopted from Section 3. Then, we study the performance of the channel access algorithms designed in Sections 4 and 5 in terms of achievable throughput.

In the throughput analysis, we consider an UW-ASN of ocean-bottom sensor nodes deployed over an area of 3000×3000 m^2. The number of source-destination pairs is set to $N = 2,\ 4,\ 6,\ 8,\ 10$. The positions of the nodes are generated randomly with the distance for each communicating pair varying in $[1000,\ 1500]$ meters in the simulation. In the testbed validation of the interference model, the distances between the transmitter and the receiver varies from 120 m to 160 m. The number of jointly optimized time slots is set to $K = 1$ to 15 with a step of 2. The number of measurement points in each time slot is set to $L = 1,\ 2,\ 3$ in the L-measurement-based interference modeling method. We consider a narrow-band UW-ASN with bandwidth of 0.5 kHz at central carrier frequency 10 kHz.[5] The modulation scheme is set to BPSK, raised-cosine filter with roll-off factor of $\beta = 0.5$ is used for pulse shaping, $\mathrm{BCH}(511,\ 259)$ is selected as the channel coding corresponding to coding rate 0.5, and $\mathrm{CRC}-16$ is adopted for parity check. PN sequences are used for packet synchronization and interference estimation (as discussed at the end of Section 4). Specifically, we consider PN sequences of duration 25 ms. In the case of $L > 1$, i.e., the interference is measured more than one time in each time slot, L PN sequences need to be inserted into a time slot. This results in a time slot duration of roughly $1 + 0.025L$ s and raw data service rate of $R_{\mathrm{svc}} = \frac{259-16}{1+0.025L}$ bits/s. The data arrival rate (in bits/s) is set to $R_{\mathrm{arv}} = \rho R_{\mathrm{svc}}$ with ρ increases from 0.1 to 2 with a step of 0.2.

Four schemes are implemented for performance comparison: i) *Centralized multi-slot channel access (Centralized Multi-slot)* as an upper bound, obtained using the developed centralized solution algorithm in Section 5 with optimality precision $\varepsilon = 0.95$ and maximum iteration number 5000; ii) *Aloha with centralized optimizer (Centralized Aloha)* as a performance bottom line, with transmission probability set to be 1 in each time slot to highlight the effects of statistical interference—Aloha with the optimal transmission probability is also considered as a special case of the centralized solution algorithm; iii) *Without Queueing (w/o Queueing)*, which corresponds to the distributed solution algorithm without considering the queueing behavior; and iv) *Single Interference Measurement (Single Meas.)*, which uses only one single measurement point to represent the interference level for a whole time slot.

Interference Model Validation. We conducted underwater interference measurement in Lake LaSalle at the University at Buffalo using six Telesonar SM-75 SMART modems by Teledyne Benthos [53]. The actual deployment of the six underwater acoustic modems is shown in Fig. 6a, with six orange buoys floating on the surface of the lake, each attached to the Telesonar SM-75 modem along with an anchor. The modem uses an omnidirectional transducer that operates in the $9\mathrm{kHz}-14\mathrm{kHz}$ low frequency (LF) band. The waveform-play feature of the modem enables transmissions of baseband complex data with a bandwidth of 5.120 kHz sampled at 10.240 kHz. The data packets were generated offline using direct-sequence CDMA (DS-CDMA) modulation scheme, and converted into a stereo WAV file in 16 bit format, and uploaded on the modems through the RS-232 interface. DS-CDMA chip waveforms were selected from the columns of a Sylvester-Hadamard matrix of order $L = 32$. Pulse shaping was done using square-root raised-cosine with roll-off factor $\beta = 0.5$ and a chip rate of $R_c = 2,048\mathrm{chips/s}$ was generated. The six modems were deployed at a depth of 2m above the lake floor in the locations shown in Fig. 6b. The distances Alice-to-Dave, Bob-to-Dave, Charlie-to-Dave, Erin-to-Dave and Frank-to-Dave were set to approximately $d_{AD} = 160\mathrm{m}, d_{BD} = 165\mathrm{m}, d_{CD} = 170\mathrm{m}, d_{ED} = 155\mathrm{m}$ and $d_{FD} = 120\mathrm{m}$, respectively. Each experiment was repeated 20 times with fixed transmit power level of 9W.[6] It is worth pointing out that, in the experimental setting considered

5. In this work, we consider a narrow-band UW-ASN, so that the resulting underwater channel is frequency-non-selective. In the case of wideband channels, the spectrum can be divided into a set of subchannels and the proposed stochastic channel access scheme can be applied to the subchannels independently.

6. The histogram were plotted as follows. Using the received data samples, we divide the magnitude of the received signal into 128 bins. In this example, the first bin is from 0 to 0.0015, the second bin is from 0.0015 to 0.003, etc. To plot the histogram i.e., the probability density function, we count the number of samples of the received data samples magnitude that lie within each bin. The resulting plot is the histogram of the received data samples. Since we have a large collection of data samples from each experiment, we can plot even much denser histogram i.e., using larger bin size with smaller bin separation.

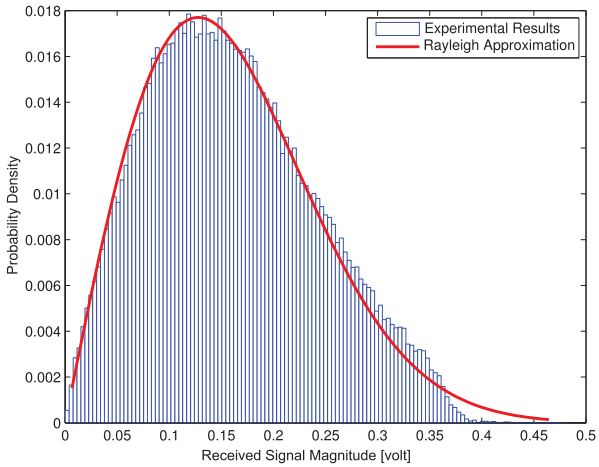

Fig. 7. Approximation of single user signal pdf using a Rayleigh distribution function in shallow water environment.

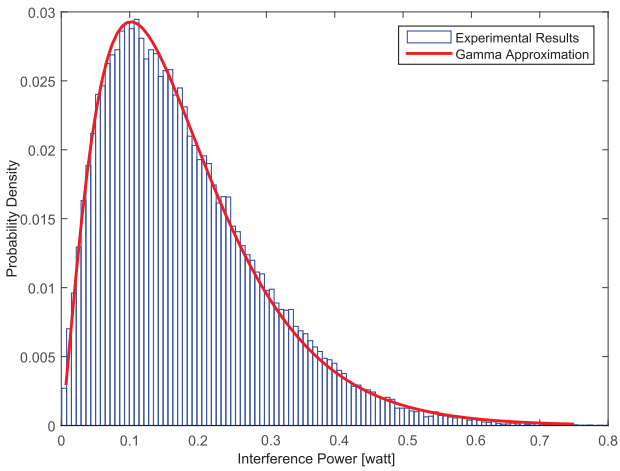

Fig. 8. Approximation of multiuser interference pdf using a Gamma distribution function in shallow water environment.

the resulting interference may be much higher than the noise. Extending the interference model to underwater environments where noise is dominant or comparable with the interference is left for future work.

Initially, Alice was selected to transmit her packet to Dave. Fig. 7 plots the probability density function (pdf) of the received signal at Dave. We can observe that the pdf can be accurately approximated by a Rayleigh distribution.

In the next set of experiments, Alice, Bob, Charlie, Erin and Frank were selected to transmit their packets P_A, P_B, P_C, P_E, and P_F to Dave, respectively, with a channel access probability of 60 percent at each time slot with a duration of $10\,\mathrm{sec}$. At each time slot on average Dave received three interfering packets. A laptop, on an inflatable boat, was used to coordinate the transmissions of the packets through a serial port interface. Dave was equipped with a data recorder that has a storage capacity of $64\mathrm{GBytes}$. The raw data were recorded and analyzed offline. The average values are presented in the plots. The pdf function of the superimposed interfering signals received at Dave is shown in Fig. 8. We can observe that the sum interference signal pdf can be approximated using a Gamma distribution function, which verifies the theoretical results. It is worth pointing out that while we consider Gamma distribution for the aggregate interference in this work, the proposed stochastic channel access scheme is not restricted to any specific channel models.

Queueing Model Verification. In Fig. 9a, we compare the original packet service time distribution $\mathrm{P}[\nu_n = z]$ with the exponential distribution $\widetilde{\mathrm{P}}[\nu_n = z]$ based on (17) and (18). The number of time slots in each frame is set to 15, with the transmission probability profiles corresponding to average transmission rate of $2.5\,\mathrm{packets/frame}$, $5\,\mathrm{packets/frame}$ and $7.5\,\mathrm{packets/frame}$. We can see that the exponential distribution gives an acceptable approximation of the original distribution in the case of low average transmission rate (top figure); as the transmission rate increases (middle and the bottom figures), the service probability is more underestimated. In the latter case, we further plot the resulting packet drop rate by considering different buffer length in Fig. 9b, where ρ is defined as the ratio of the incoming and outgoing packet rate. We can see that the truncated $M/M/1$ fits the measured packet drop rate very well. In Fig. 9c, we further plot the accumulative queue length achieved by the original queue model and the truncated $M/M/1$ in 1000 time slots. We can see that the two models coincide well with each other.

Throughput. Sum throughput against the number of jointly optimized time slots is plotted in Fig. 10 with four source-destination pairs. We observe that considerable improvement can be achieved by jointly optimizing the transmission strategy over a group of time slots. For example, in the case of $T = 5,\ 7,\ 9$, i.e., when the number of jointly optimized time slots is larger than the number of concurrent users (4 in

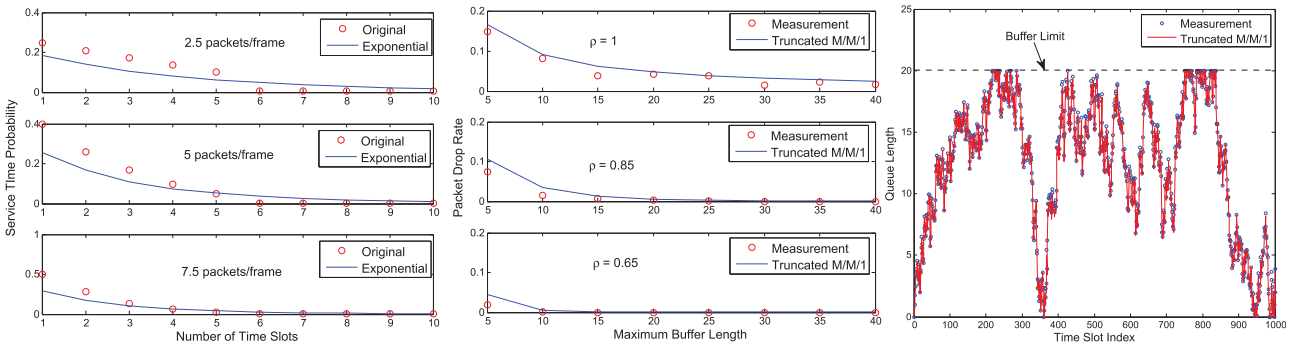

Fig. 9. Queue approximation using a truncated $M/M/1$ queueing model: (a) service rate, (b) packet drop rate, and (c) an example of accumulative queue length.

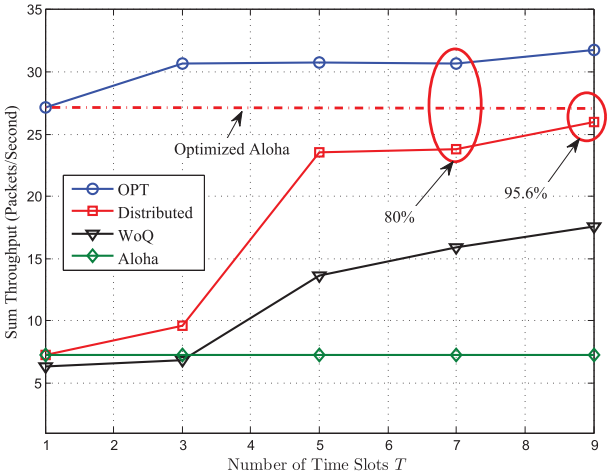

Fig. 10. Sum throughput against the number of jointly optimized time slots.

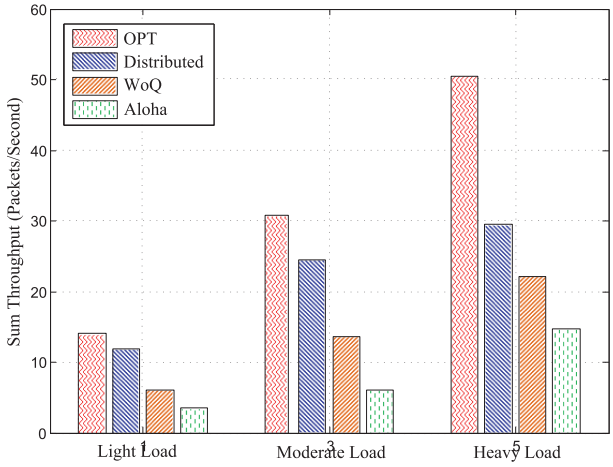

Fig. 12. Sum throughput achieved in the case of different traffic loads.

this simulation), a throughput around 25 packets/second can be achieved by the proposed distributed solution algorithm, which is 3.5 times higher than that of *Aloha*, and 80 percent of the global optimum. In the case of $T = 1$, the centralized optimal solution algorithm reduces to Aloha with network-wide optimized transmission probability (which is not easy to determine in distributed manner). We also observe that a throughput level very close to that of the optimized Aloha can be achieved by distributed channel access, i.e., higher than 95 percent with 9 time slots jointly considered. When the queueing behavior of users is not considered, a noticeable throughput gain can still be achieved compared to Aloha when $T \geq 4$. However, compared to queueing-aware channel access, the throughput gain reduces from 3.5 times to 2 for $T = 5$ and to 2.5 for $T = 9$, respectively.

In Fig. 11, we evaluate the performance of the proposed distributed algorithm with number of users N varied from 2 to 10 while the number of jointly optimized time slots is set to 5. We observe that the proposed distributed solution algorithm consistently outperforms *WoQ* and *Aloha*. For example, in the case of 4 users, a sum throughput of 25 can be achieved by *Distributed* while only less than 15 and around 7 can be achieved by *WoQ* and *Aloha*. In the case of 6 users, a sum throughput of 17 can be achieved by *Distributed*, which is around 3 times higher than the throughput achieved by *WoQ* and *Aloha*. It is worth pointing out that, unsurprisingly, as the number of users increases, the price of anarchy caused by the lack of a centralized controller can be very large, e.g., in the case of 10 users, only less than 10 percent of the global optimum can be achieved through distributed, uncoordinated algorithms with no message exchange. This implies that the network becomes severely congested with high number of concurrent users, and it is not so effective any more to increase the number of jointly optimized time slots only. Additional experiments considering 8 users and 8 time slots indicate that, the resulting sum throughput only slightly increases (from 8 to 9.5) compared to the case of 5 time slots. A possible solution is to introduce partial cooperation among interfering users, e.g., design distributed solution algorithms based on pricing strategies [60]; this will be the subject of our future work.

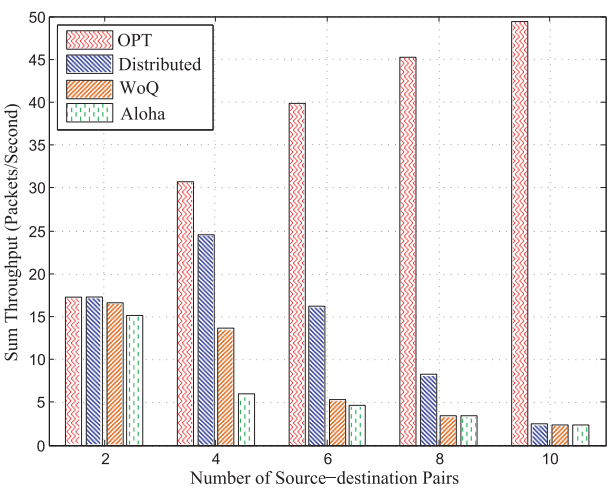

Fig. 11. Sum throughput achieved in the case of different users.

In Fig. 12, the sum throughput of the proposed distributed algorithm is reported with 4 users, 5 time slots, against different offered traffic loads: light, moderate and heavy, corresponding to average data arrival rate smaller than, comparable to and higher than the data transmission rate, respectively. We observe that a sum throughput close to the global optimum can be achieved by the proposed distributed channel access in the former two cases, while only 60 percent of the global optimum can be achieved in the third case. Performance degradation is due to the fact that, with heavier traffic, each user prefers to transmit more often to avoid high packet loss rates due to violating the delay constraint, which results in higher level of network interference overall. Again, in this case, partial cooperation among interfering users might be helpful for efficient MAC protocol design.

The advantages of the L-measurement-based interference modeling method are illustrated in Fig. 13 through performance comparison between *Distributed* and *SM* in the case of four source-destination pairs, i.e., $N = 4$. Much higher throughput can be achieved by *Distributed* than *SM* with the number of time slots larger than N. For example, with $T = 5$, a sum throughput close to 25 can be achieved by *Distributed*, which is over three times as high as the sum-throughput of *SM*. This verifies that, by representing the interference level in each time slot based on multiple measurement points, the

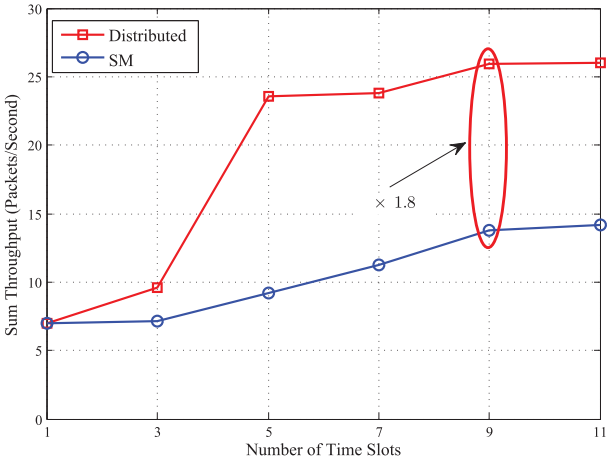

Fig. 13. Sum throughput achieved by *Distributed* and *SM* against the number of jointly considered time slots.

statistical behavior of interference with both spatial and temporal uncertainty can be modeled more precisely, and hence each transmitter has more flexibility in optimally adapting its own probabilistic transmission strategy profile to avoid interference from other transmitters.

7 Conclusion

We have studied a stochastic, distributed and asynchronous channel access scheme for underwater acoustic networks in which each transmitter optimizes a transmission probability profile based on which it decides whether to transmit or to enqueue its packets over a series of time slots *based on a statistical characterization of interference* obtained from past observations. To capture the effects of temporal uncertainty of interference, we proposed an L-measurement method to model the effect of unaligned interference at a receiver. At each measurement, the multi-user interference is modelled using a Gamma distribution function. We validated through testbed experiments that the model can capture the statistical characteristics of interference in shallow water environments very well. We presented a mathematical formulation and solution algorithms for the problem of dynamic transmission strategy optimization. Results have shown that considerable improvement in sum-throughput can be achieved by jointly optimizing over multiple time slots. In future research, we will study the distributed network control problems based on noncooperative game theory [60], [61], test the proposed stochastic channel access protocols in terms of end-to-end throughput and delay over testbed experiments. Another research direction is to compare the proposed stochastic channel access protocol with existing protocols through a comprehensive experimentation campaign in real underwater environments.

Acknowledgments

This work was supported in part by the National Science Foundation under Grant CNS-1763709 and Grant CNS-1726512. A preliminary shorter version of this paper appeared in the Proceedings of the ACM International Conference on UnderWater Networks and Systems (WUWNet), Los Angeles, CA, USA, November 5-6, 2012 [1].

References

[1] Z. Guan, T. Melodia, and D. Yuan, "Stochastic channel access for underwater acoustic networks with spatial and temporal interference uncertainty," in *Proc. ACM Int. Conf. UnderWater Netw. Syst.*, 2012, Art. no. 18.

[2] T. Melodia, H. Kulhandjian, L. Kuo, and E. Demirors, "Advances in underwater acoustic networking" in *Mobile Ad Hoc Networking: Cutting Edge Directions*, S. Basagni, M. Conti, S. Giordano and I. Stojmenovic Eds., 2nd ed., Hoboken, NJ, USA: Wiley, 2013.

[3] J. Proakis, E. Sozer, J. Rice, and M. Stojanovic, "Shallow water acoustic networks," *IEEE Commun. Magazine*, vol. 39, no. 11, pp. 114–119, Nov. 2001.

[4] H. Kulhandjian and T. Melodia, "A low-cost distributed networked localization and time-synchronization framework for underwater acoustic testbeds," in *Proc. IEEE Underwater Commun. Conf. Workshop*, 2014, pp. 1–5.

[5] A. Syed, W. Ye, J. Heidemann, and B. Krishnamachari, "Understanding spatio-temporal uncertainty in medium access with ALOHA protocols," in *Proc. ACM Int. Workshop UnderWater Netw.*, 2007, pp. 41–48.

[6] H. Kulhandjian and T. Melodia, "Modeling underwater acoustic channels in short-range shallow water environments," in *Proc. ACM Int. Conf. UnderWater Netw. Syst.*, 2014, Art. no. 26.

[7] A. A. Syed, W. Ye, and J. Heidemann, "Comparison and evaluation of the T-Lohi MAC for underwater acoustic sensor networks," *IEEE J. Sel. Areas Commun.*, vol. 26, no. 9, pp. 1731–1743, Dec. 2008.

[8] B. Peleato and M. Stojanovic, "Distance aware collision avoidance protocol for Ad-Hoc underwater acoustic sensor networks," *IEEE Commun. Lett.*, vol. 11, no. 12, pp. 1025–1027, Dec. 2007.

[9] X. Guo, M. Frater, and M. Ryan, "Design of a propagation-delay-tolerant MAC protocol for underwater acoustic sensor networks," *IEEE J. Oceanic Eng.*, vol. 34, no. 2, pp. 170–180, Apr. 2009.

[10] M. Chitre, M. Motani, and S. Shahabudeen, "Throughput of networks with large propagation delays," *IEEE J. Oceanic Eng.*, vol. 37, no. 4, pp. 645–658, Oct. 2012.

[11] Z. Zhou, Z. Peng, J.-H. Cui, and Z. Jiang, "Handling triple hidden terminal problems for multichannel MAC in long-delay underwater sensor networks," *IEEE Trans. Mobile Comput.*, vol. 11, no. 1, pp. 139–154, Jan. 2012.

[12] J. Jagannath, A. Saji, H. Kulhandjian, Y. Sun, E. Demirors, and T. Melodia, "A hybrid MAC protocol with channel-dependent optimized scheduling for clustered underwater acoustic sensor networks," in *Proc. ACM Int. Conf. UnderWater Netw. Syst.*, 2013, pp. 1–8.

[13] H.-H. Ng, W.-S. Soh, and M. Motani, "An underwater acoustic MAC protocol using reverse opportunistic packet appending," *Comput. Netw.*, vol. 57, no. 14, pp. 2733–2751, Oct. 2013.

[14] L. Jin and D. D. Huang, "A slotted CSMA based reinforcement learning approach for extending the lifetime of underwater acoustic wireless sensor networks," *Comput. Commun.*, vol. 36, no. 9, pp. 1094–1099, May 2013.

[15] M. Biagi, S. Rinauro, and R. Cusani, "UWA interference analysis for cognitive access," in *Proc. MTS/IEEE OCEANS*, 2013, pp. 1–5.

[16] Y. Sun and T. Melodia, "The internet underwater: An IP-compatible protocol stack for commercial undersea modems," in *Proc. ACM Int. Conf. UnderWater Netw. Syst.*, 2013, pp. 1–8.

[17] S. Misra, S. Dash, M. Khatua, A. V. Vasilakos, and M. Obaidat, "Jamming in underwater sensor networks: Detection and mitigation," *IET Commun.*, vol. 6, no. 14, pp. 2178–2188, Sep. 2012.

[18] L. Zhang, Z. Guan, and T. Melodia, "Cooperative anti-jamming for infrastructure-less wireless networks with stochastic relaying," in *Proc. IEEE Int. Conf. Comput. Commun.*, 2014, pp. 549–557.

[19] H. X. Tan and W. K. G. Seah, "Distributed CDMA-based MAC protocol for underwater sensor networks," in *Proc. 32nd IEEE Conf. Local Comput. Netw.*, 2007, pp. 26–36.

[20] D. Pompili, T. Melodia, and I. F. Akyildiz, "A CDMA-based medium access control protocol for underwater acoustic sensor networks," *IEEE Trans. Wireless Commun.*, vol. 8, no. 4, pp. 1899–1909, Apr. 2009.

[21] L.-C. Kuo and T. Melodia, "Distributed medium access control strategies for MIMO underwater acoustic networking," *IEEE Trans. Wireless Commun.*, vol. 10, no. 8, pp. 2523–2533, Aug. 2011.

[22] L. Badia, M. Mastrogiovanni, C. Petrioli, S. Stefanakos, and M. Zorzi, "An optimization framework for joint sensor deployment, link scheduling and routing in underwater sensor networks," in *Proc. ACM Int. Workshop UnderWater Netw.*, 2006, pp. 56–63.

[23] P. Mandal and S. De, "A new dynamic reservation protocol for many-to-one multi-access with long propagation delay," in *Proc. IEEE Veh. Technol. Conf.*, 2012, pp. 1–5.
[24] G. Fan, H. Chen, L. Xie, and K. Wang, "A hybrid reservation-based MAC protocol for underwater acoustic sensor networks," *Ad Hoc Netw.*, vol. 11, no. 3, pp. 1178–1192, May 2013.
[25] K. Kredo II , P. Djukic, and P. Mohapatra, "Stump: Exploiting position diversity in the staggered TDMA underwater MAC protocol," in *Proc. IEEE Int. Conf. Comput. Commun.*, 2009, pp. 2961–2965.
[26] C. Yun and Y.-K. Lim, "GSR-TDMA: A geometric spatial reuse-time division multiple access MAC protocol for multihop underwater acoustic sensor networks," *J. Sensors*, vol. 2016, 2016, Art. no. 6024610.
[27] X. Pan, J. Cui, and J. Liu, "A MAC protocol design for underwater acoustic WiFi network," in *Proc. ACM Int. Conf. Underwater Netw. Syst.*, 2018, pp. 1–2.
[28] H. Mei, H. Wang, X. Shen, and W. Bai, "An adaptive MAC protocol for underwater acoustic sensor networks with dynamic traffic," in *Proc. MTS/IEEE Charleston*, 2018, pp. 1–4.
[29] F. Alfouzan, A. Shahrabi, S. M. Ghoreyshi, and T. Boutaleb, "An energy-conserving depth-based layering MAC protocol for underwater sensor networks," in *Proc. Veh. Technol. Conf.*, 2018, pp. 1–6.
[30] F. Bouabdallah, C. Zidi, R. Boutaba, and A. Mehaoua, "Collision avoidance energy efficient multi-channel MAC protocol for underwater acoustic sensor networks," *IEEE Trans. Mobile Comput.*, vol. 18, no. 10, pp. 2298–2314, Oct. 2019.
[31] N. Morozs, P. D. Mitchell, and Y. Zakharov, "Dual-Hop TDA-MAC and routing for underwater acoustic sensor networks," *IEEE J. Oceanic Eng.*, vol. 44, no. 4, pp. 865–880, Oct. 2019.
[32] N. Morozs, P. D. Mitchell, and Y. Zakharov, "Linear TDA-MAC: Unsynchronized scheduling in linear underwater acoustic sensor networks," *IEEE Netw. Lett.*, vol. 1, no. 3, pp. 120–123, Sep. 2019.
[33] R. Zhao, H. Long, O. A. Dobre, X. Shen, T. M. N. Ngatched, and H. Mei, "Time reversal based MAC for multi-hop underwater acoustic networks," *IEEE Syst. J.*, vol. 13, no. 3, pp. 2531–2542, Sep. 2019.
[34] X. Zhuo, F. Qu, H. Yang, and Y. Wu, "Time-based adaptive collision-avoidance real-time MAC protocol for underwater acoustic sensor networks," in *Proc. ACM Int. Conf. Underwater Netw. Syst.*, 2018, pp. 1–5.
[35] H. Kulhandjian, T. Melodia, and D. Koutsonikolas, "CDMA-based analog network coding for underwater acoustic sensor networks," *IEEE Trans. Wireless Commun.*, vol. 14, no. 11, pp. 6495–6507, Nov. 2015.
[36] S. Jiang, "On reliable data transfer in underwater acoustic networks: A survey from networking perspective," *IEEE Commun. Surveys Tuts.*, vol. 20, no. 2, pp. 1036–1055, Second Quarter 2018.
[37] M. Jouhari, K. Ibrahimi, H. Tembine, and J. Ben-Othman, "Underwater wireless sensor networks: A survey on enabling technologies, localization protocols, and internet of underwater things," *IEEE Access*, vol. 7, pp. 96 879–96 899, Jul. 2019.
[38] D. Marinakis, K. Wu, N. Ye, and S. Whitesides, "Network optimization for lightweight stochastic scheduling in underwater sensor networks," *IEEE Trans. Wireless Commun.*, vol. 11, no. 8, pp. 2786–2795, Aug. 2012.
[39] K. Patil, M. Jafri, D. Fiems, and A. Marin, "Stochastic modeling of depth based routing in underwater sensor networks," *Ad Hoc Netw.*, vol. 89, pp. 132–141, 2019.
[40] Y. Han, Y. Fei, and A. Ding, "SMARP: A stochastic MAC protocol with randomized power control for underwater sensor networks," in *Proc. 13th Annu. IEEE Int. Conf. Sens. Commun. Netw.*, 2016, pp. 1–9.
[41] M. Rahmati and D. Pompili, "Probabilistic spatially-divided multiple access in underwater acoustic sparse networks," *IEEE Trans. Mobile Comput.*, vol. 19, no. 2, pp. 405–418, Feb. 2020.
[42] D. Marinakis, K. Wu, and S. Whitesides, "Stochastic scheduling for underwater sensor networks," in *Proc. Int. Conf. Res. Netw.*, 2011, pp. 134–146.
[43] S. Lu, Z. Wang, Z. Wang, and S. Zhou, "Throughput of underwater wireless ad hoc networks with random access: A physical layer perspective," *IEEE Trans. Wireless Commun.*, vol. 14, no. 11, pp. 6257–6268, Nov. 2015.
[44] A. Stefanov and M. Stojanovic, "Performance analysis of underwater acoustic random access networks," in *Proc. Int. Symp. Problems Redundancy Inf. Control Syst.*, 2012, pp. 84–88.
[45] R. J. Urick, *Principles of Underwater Sound*. New York, NY, USA: McGraw-Hill, 1983.
[46] F. Fisher and V. Simmons, "Sound absorption in sea water," *J. Acoustical Soc. America*, vol. 62, no. 3, pp. 558–564, Sep. 1977.
[47] D. Pompili, T. Melodia, and I. F. Akyildiz, "A CDMA-based medium access control protocol for underwater acoustic sensor networks," *IEEE Trans. Wireless Commun.*, vol. 8, no. 4, pp. 1899–1909, Apr. 2009.
[48] N. S. N. Ismail, L. A. Hussein, and S. H. Ariffin, "Analyzing the performance of acoustic channel in underwater wireless sensor network (UWSN)," in *Proc. IEEE Asia Int. Conf. Math./Anal. Modelling Comput. Simul.*, 2010, pp. 550–555.
[49] F. Bouabdallah and R. Boutaba, "A distributed OFDMA medium access control for underwater acoustic sensors networks," in *Proc. IEEE Int. Conf. Commun.*, 2011, pp. 1–5.
[50] V. Krishnaswamy and S. S. Manvi, "Analysis of acoustic channel in underwater acoustic sensor network," in *Proc. IEEE Int. Advance Comput. Conf.*, 2015, pp. 233–236.
[51] R. K. Ganti and M. Haenggi, "Interference and outage in clustered wireless Ad Hoc networks," *IEEE Trans. Inf. Theory*, vol. 55, no. 9, pp. 4067–4086, Sep. 2009.
[52] R. W. H. Jr, M. Kountouris, and T. Bai, "Modeling heterogeneous network interference using poisson point processes," *IEEE Trans. Signal Process.*, vol. 61, no. 16, pp. 4114–4126, Aug. 2013.
[53] Teledyne-Benthos, Acoustic Modems. 2010. [Online]. Available: http://www.benthos.com
[54] A. Goldsmith, *Wireless Communications*. Cambridge, U.K.: Cambridge Univ. Press, 2004.
[55] L. Lipsky, *Queueing Theory: A Linear Algebraic Approach*, 2nd ed. New York, NY, USA: Springer, 2008.
[56] S. Boyd and L. Vandenberghe, *Convex Optimization*. Cambridge, U.K.: Cambridge Univ. Press, 2004.
[57] S. Boyd and J. Mattingley, "Branch and Bound Methods," Stanford, CA, USA: Stanford Univ., Mar. 2007.
[58] I. P. Androulakis, "MINLP: Branch and bound global optimization algorithm," *Encyclopedia Optim.*, pp. 1415–1421, 2011.
[59] H. D. Sherali and W. P. Adams, *A Reformulation-Linearization Technique for Solving Discrete and Continuous Nonconvex Problems*. Boston: MA, USA: Kluwer Academic, 1999.
[60] Z. Guan, T. Melodia, and G. Scutari, "Distributed queuing games in interference-limited wireless networks," in *Proc. IEEE Int. Conf. Commun.*, 2013, pp. 1810–1815.
[61] T. Basar and G. J. Olsder, *Dynamic Noncooperative Game Theory (Classics in Applied Mathematics)*. Philadelphia, PA, USA: Society for Industrial and Applied Mathematics, 1999.

Zhangyu Guan (Member, IEEE) received the PhD degree in communication and information systems from Shandong University, in China, in 2010. He is currently an assistant professor with the Department of Electrical Engineering, State University of New York at Buffalo, where he directs the Wireless Intelligent Networking and Security (WINGS) Lab, with research interests including network design automation, new spectrum technologies, and wireless network security. He has served as an area editor for Elsevier Journal of Computer Networks since July 2019. He has served as TPC chair for IEEE INFOCOM Workshop on Wireless Communications and Networking in Extreme Environments (WCNEE) 2020, Student Travel Grants Chair for IEEE Sensor, Mesh and Ad Hoc Communications and Networks (SECON) 2019-2020, Information System (EDAS) Chair for IEEE Consumer Communications Networking Conference (CCNC) 2021. He has also served as TPC member for IEEE INFOCOM 2016-2020, IEEE GLOBECOM 2015-2020, IEEE MASS 2017-2019, IEEE IPCCC 2015-2019, among others.

Hovannes Kulhandjian (Senior Member, IEEE) received the BS degree (magna cum laude) in electronics engineering from the American University, in Cairo, Cairo, Egypt, in 2008, and the MS and PhD degrees in electrical engineering from the State University of New York at Buffalo, Buffalo, NY, in 2010 and 2014, respectively. From December 2014 to July 2015, he was an associate research engineer with the Department of Electrical and Computer Engineering, Northeastern University, Boston, MA. He is currently an assistant professor with the Department of Electrical and Computer Engineering, California State University, Fresno, Fresno, CA. His current research interests include wireless communications and networking, with applications to underwater acoustic communications, visible light communications and applied machine learning. He has served as a guest editor for IEEE Access - Special Section Journal on Underwater Wireless Communications and Networking. He has also served as a session co-chair for IEEE UComms 2020, session chair for ACM WUWNet 2019. He actively serves as a member of the Technical Program Committee for ACM and IEEE conferences such as IEEE GLOBECOM 2015-2020, UComms 2020, PIMRC 2020, WD 2019, ACM WUWNet 2019, ICC 2015-2018, among others.

Tommaso Melodia (Fellow, IEEE) received the PhD degree in electrical and computer engineering from the Georgia Institute of Technology, in 2007. He is currently the William Lincoln Smith professor with the Department of Electrical and Computer Engineering, Northeastern University. He is also the director of the Institute for the Wireless Internet of Things, and the director of research for the PAWR Project Office, a public-private partnership that is developing four city-scale platforms for advanced wireless research in the United States. His research focuses on modeling, optimization, and experimental evaluation of wireless networked systems, with applications to 5G networks and Internet of Things, software-defined networking, and body area networks. His research is supported mostly by the U.S. federal agencies, including the National Science Foundation, the Air Force Research Laboratory, the Office of Naval Research, the Army Research Laboratory, and DARPA. He is a senior member of the ACM. He is the editor-in-chief of Computer Networks, and a former associate editor of the *IEEE Transactions on Wireless Communications*, the *IEEE Transactions on Mobile Computing*, the *IEEE Transactions on Multimedia*, among others.